Adaptive Noise Removal IRF-RETROICOR

E. B. Beall[1], and M. J. Lowe[1]
[1]Radiology, Cleveland Clinic, Cleveland, OH, United States

Introduction: It has become common to correct for physiologic noise by prior regression [1] or by inclusion in the fit model for BOLD-weighted functional connectivity (fcMRI) and in some cases, for fMRI[2-4]. The noise model is based on the RETROICOR model [5,1], which removes variance with the same quasi-periodicity as the cardiac and respiratory cycles. However, to model the noise accurately, a large number of regressors is needed. For example, RET-2 (hereafter RETROICOR will be referred to as RET-N where N is model order) requires 2 orders of sine and cosine for both cardiac and respiration, or 8 regressors. In some applications at 3 Tesla, orders up to RET-5 have been shown to be necessary, but 5th order requires 20 regressors. It is a known issue (but not always accounted for) that increasing the number of regressions in a correction reduces the statistical power of the corrected dataset (see Fig 1b for std dev versus correction with simulated phase and increasing RET model order). Furthermore, it is our hypothesis that a more parsimonious model based on the most-strongly fitted noise signatures can explain all of the cardiac and respiration noise variance. We show a modification to RETROICOR that removes the same significantly fitted variance as RET-5 but with only 6 regressors (4 for cardiac, 2 for respiration), less than RET-2. We show evidence in 34 subjects that the cardiac and respiratory noise signatures detected by our methods are very similar across subjects, implying these are the actual noise signatures, and recommend adaptive noise modeling when the model order is greater than 2.

Adaptive RETROICOR: IRF-RET: The RETROICOR model is shown in Eqn 1, where theta$_{c,r}$ are physiologic phase, a,b$_{c,r}$ are fit coefficients and s$_{c,r}$ are the modeled noise signals as described in [1]. This is fitted at every voxel (see Fig 1a for phase and RET-2 fit to pulse plethysmograph signal) to obtain coupling coefficients a,b, and are also normalized by variance as $t_{c,r}$ as in Eqn 2,3 by performing a vector sum and dividing by the non-modeled standard deviation. Simulated coupling t_{sim} is determined for each dataset using Monte Carlo method of inputting random phase for theta. This gives us the null distribution of coupling. These are both histogrammed as in Fig 1c and **coupling power** for card, resp in each model is assessed as the percentage of voxels with greater t_c or t_r than t_{sim}.

$$s_{c,r} = \sum_{i}^{N}\left[a_{c,r}\sin(i\times\theta_{c,r}) + b_{c,r}\cos(i\times\theta_{c,r})\right] \quad \text{Eqn 1,} \qquad P_{c,r} = \sqrt{\sum_{i}^{N}\left(a_{c,r}^2 + b_{c,r}^2\right)} \quad \text{Eqn 2,} \qquad t_{c,r} = \frac{P_{c,r}}{\sigma} \quad \text{Eqn 3}$$

We introduce our usage of the term "impulse response" as describing the peak-to-peak shape of the temporal signature of s_c and s_r (cardiac and respiratory are handled separately after this point) over one cycle, which under the traditional model are different for every voxel. The coupling coefficients for all significantly coupled voxels (significance determined using Eqns 1-3 in Monte Carlo method) are converted into impulse responses by creating a phase timeseries theta from 0 to 2pi and passing to Eqn 1. These are weighted by the coupling power, and passed to a principal component analysis (PCA) to determine if a small subset explains most of them (the PCA returns components ranked by variance explained, so they are also ranked in order of coupling). These are then regressed in parallel at every voxel and the fit t-statistics are thresholded. Those that explain a significant part of the variance are kept as our impulse response functions (IRFs). In preliminary investigations, the first 4 cardiac and first 2 respiratory IRFs were selected. The regression and removal of these is termed IRF-RETROICOR (or IRF-RET).

Methods: 34 subjects were scanned at 3T with 12-ch receive head coil with: 1) anatomic whole-brain T1, 2) BOLD-weighted EPI, block-paradigm complex finger tapping fMRI for 156 volumes, 3) EPI, resting state fcMRI for 132 volumes. Both EPI scans were 128x128x31 matrix, 2x2x4mm voxels, TE/TR=29/2800. The MPRAGE and EPI datasets were passed to the PESTICA tool [6] to obtain pulse and respiration estimators. Pulse and respiration was also recorded in parallel for scan 3, which was found to have identical periodicity as the estimators for every subject. For all subsequent analyses, PESTICA estimators were used as input to RET and IRF-RET for scan 2 and 3. Data was either corrected using RET or IRF-RET and the **coupling power** (Eqn 3) was averaged for all in-brain voxels. The corrections correspond to 8, 20, and 6 regressors, for RET-2, RET-5 and IRF-RET respectively. Datasets corrected with IRF-RET were subsequently passed to RET and the coupling to RET-2 and RET-5 determined as the **residual coupling power** after IRF-RET. The IRFs determined in the adaptive methods for each dataset were compared across subjects by **mean IRF correlation** to average IRFs. fMRI and fcMRI were analyzed as described elsewhere [7] for activation and left primary motor cortex connectivity. **Mean standard deviation within activated voxels** for fMRI data and within **connected voxels** for fcMRI data (in each case voxels identified in data corrected with RET-2) were computed for each correction.

Results: Based on the residual coupling power (Table 1), IRF-RET removes any non-null variance associated with RET-2, 80 percent of cardiac variance associated with RET-5, and all respiratory variance in RET-5. The most consistent IRFs (shown in Fig 2 along with group averaged spatially normed coupling maps for RET-2 and IRF-RET) were remarkably consistent, with average correlations to group mean IRFs (across subjects both fMRI and fcMRI, fcMRI in parantheses) of 0.95 (0.93), 0.80(0.75), 0.79(0.76) and 0.51(0.53) for the first 4 cardiac IRFs, 0.97(0.96) and 0.92(0.94) for the first 2 respiratory IRFs. The high correlations of each lends support to a secondary hypothesis: that these IRFs are modeling the true signatures of physiologic noise. Std devs are given in Table 2 under simulated phase and PESTICA (real) phase, and shows decrease with order of correction.

	Coupling Power		Residual Coupling	
	fMRI	fcMRI	fMRI	fcMRI
RET-2-Resp	0.446	0.492	0.000	0.002
RET-2-Card	0.269	0.236	0.000	0.000
RET-5-Resp	0.345	0.379	0.000	0.003
RET-5-Card	0.163	0.138	0.032	0.027

Table 1: average total coupling and residual coupling

	IRF	RET-2	RET-5
Std Dev-Sim-fMRI	0.984	0.978	0.943
Std Dev-RET-fMRI	0.936	0.926	0.907
Std Dev-Sim-fcMRI	0.979	0.973	0.929
Std Dev-RET-fcMRI	0.909	0.898	0.873

Table 2: standard dev inside activated or connected

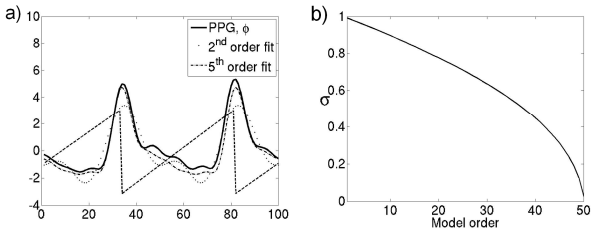

Figure 1: a) pulse plethys signal, physio phase and RET-2/5 fits, b) stddev versus RET model order, c) coupling power in dark grey as proportion of t_{real} greater than $t_{simulated}$.

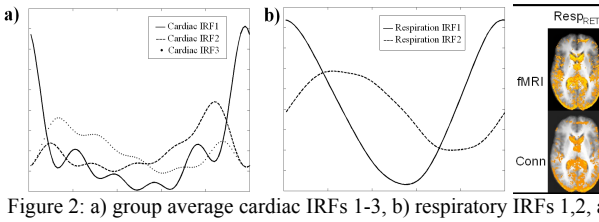

Figure 2: a) group average cardiac IRFs 1-3, b) respiratory IRFs 1,2, and average spatial coupling maps

Discussion: As model order is increased, data is effectively being thrown away and using our model preserves variance while correcting for noise fully by zeroing in on the actual signatures of the noise. This method can be used in any quasiperiodic regression based on phase, and these signatures may be useful for modeling abnormal physiology.

References: 1) Glover et al, MRM 2000;44:162-167, 2) Lund et al, Neuroimage 2006;29:54-66, 3) Brooks et al, Neuroimage 2008;39:680-692, 4) Harvey et al, JMRI 2008;28:1337-1344, 5) Hu et al, MRM 1995;34:201-212, 6) Beall et al, Neuroimage 2007;37:1286-1300, 7) Lowe et al, HBM 2008;29:818-827